Joule

CellPress

Article

Data-Driven Safety Envelope of Lithium-Ion Batteries for Electric Vehicles

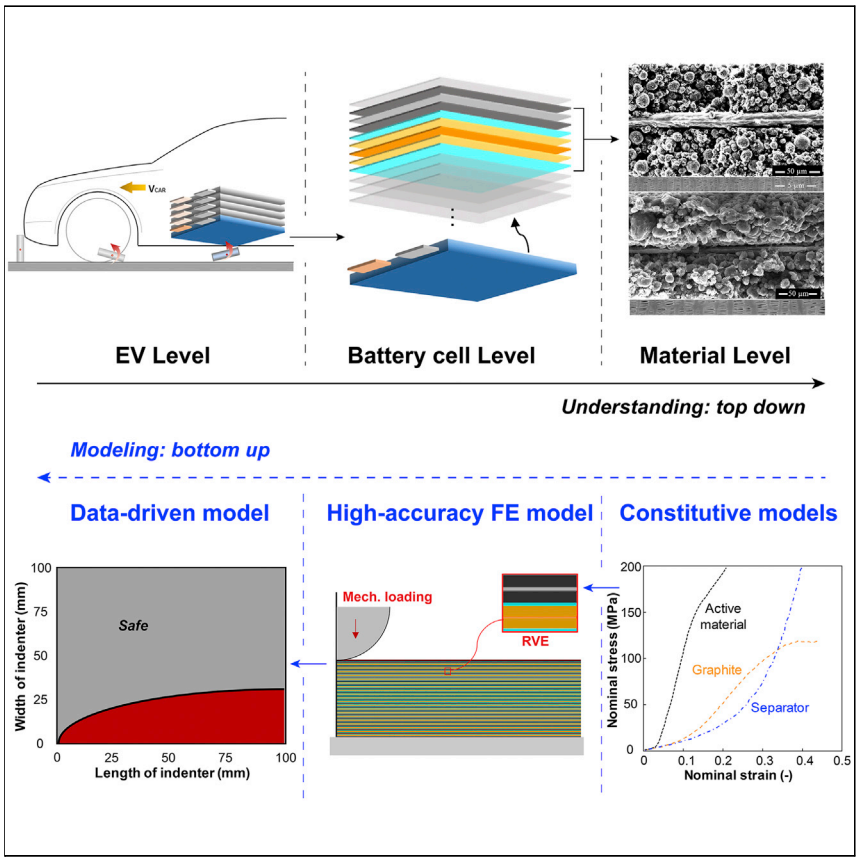

We demonstrated the use of the powerful machine learning tool to develop the "safety envelope" of lithium-ion batteries for electric vehicles that provides the range of mechanical loading conditions ensuring safe operation. The daunting challenge of obtaining a large databank of battery tests was overcome by utilizing a high-accuracy finite element model of a pouch cell to generate over 2,500 numerical simulations. The safety envelope will serve as important guidelines to the design of EV and batteries.

Wei Li, Juner Zhu, Yong Xia, Maysam B. Gorji, Tomasz Wierzbicki

zhujuner@mit.edu (J.Z.)
xiayong@tsinghua.edu.cn (Y.X.)

HIGHLIGHTS

Develops "safety envelope" of battery cells—the range ensuring safe operation

Demonstrates the application of machine learning to battery and EV safety

The use of high-accuracy computational tool to generate a large databank

Visualizes the safety envelope by two phase diagrams, a classifier, and a regressor

Li et al., Joule 3, 2703–2715
November 20, 2019 © 2019 Elsevier Inc.
https://doi.org/10.1016/j.joule.2019.07.026

Joule

CellPress

Article

Data-Driven Safety Envelope of Lithium-Ion Batteries for Electric Vehicles

Wei Li,[1,2,3] Juner Zhu,[1,3,4,*] Yong Xia,[2,*] Maysam B. Gorji,[1] and Tomasz Wierzbicki[1]

SUMMARY

In the accident scenarios of electric vehicles, the battery pack can be damaged catastrophically, resulting in the electric short circuit, thermal runaway, and possible fire and explosion. Therefore, it is important to investigate the range of conditions under which the safe operation of each individual cell is adequately controlled, known as the "safety envelope". The biggest challenge of developing such a safety envelope lies in the acquisition of a large data bank of battery failure tests. In this study, we overcome the challenge by establishing a high-accuracy detailed computational model of lithium-ion pouch cells, in which all the component materials are characterized by well-calibrated constitutive models. A large matrix of extreme mechanical loading conditions is simulated, and a data-driven safety envelope is obtained using the machine learning algorithm. This work is a demonstration of combining numerical data generation with data-driven modeling to predict the safety of energy storage systems.

INTRODUCTION

The commercialization of lithium-ion batteries has accelerated the electrification process of vehicles. Life span, cost, performance, specific energy, specific power, and safety are commonly understood as the six important guidelines of electric vehicle (EV) batteries.[1,2] The former five aspects have received a great deal of attention and achieved great improvements during the past decade,[3] but the safety has not been adequately addressed by most of the stakeholders in the EV market.

Existing safety studies mostly focus on the thermal events of battery cells and modules[4–8] as well as the innovation of safer energy materials.[9] The understanding of mechanical failure, which is one of the most likely causes of a thermal runaway, has long been a blind spot of the EV and battery community. It is disappointing that there is still no worldwide-accepted standard or regulation about battery safety tests,[10] while about half of the highly publicized fire accidents of plug-in EVs were confirmed to be caused by mechanical loadings, which could come from the collision with another vehicle or even objects from the highway, known as "ground impact,"[11] see the sketch of the impact process in Figure 1A.

There is a growing awareness of the EV OEMs as well as the consumers about the importance of such mechanical failures. In a recent perspective article,[12] researchers of Ford Motor Company called for efforts from multiple disciplines to developing mechanical models that can "accurately and efficiently predict failure conditions of batteries with different formats under different scenarios." This statement precisely describes the most urgent task of the whole community, which is the

Context & Scale

The rapid improvement of battery technology has brought the world into a new era of EV. However, the industry is now facing a new challenge in this new era—the crash safety of EV compared to its gasoline counterpart. The most urgent task is to identify the range of mechanical loading conditions ensuring safe operation of battery cells, known as the "safety envelope." To develop it requires a huge databank of mechanical tests, making it a daunting challenge. Here, we overcame this challenge by employing a high-accuracy finite element model of a pouch cell to produce over 2,500 simulations and analyzed the data with machine learning algorithms. We visualized the safety envelope with two types of phase diagrams, a classifier that fast predicts of short circuit or safe to a given loading condition and a regressor that quantitatively tells the amount of deformation needed to develop a short. The safety envelope provides important guidelines to the design of EV and batteries.

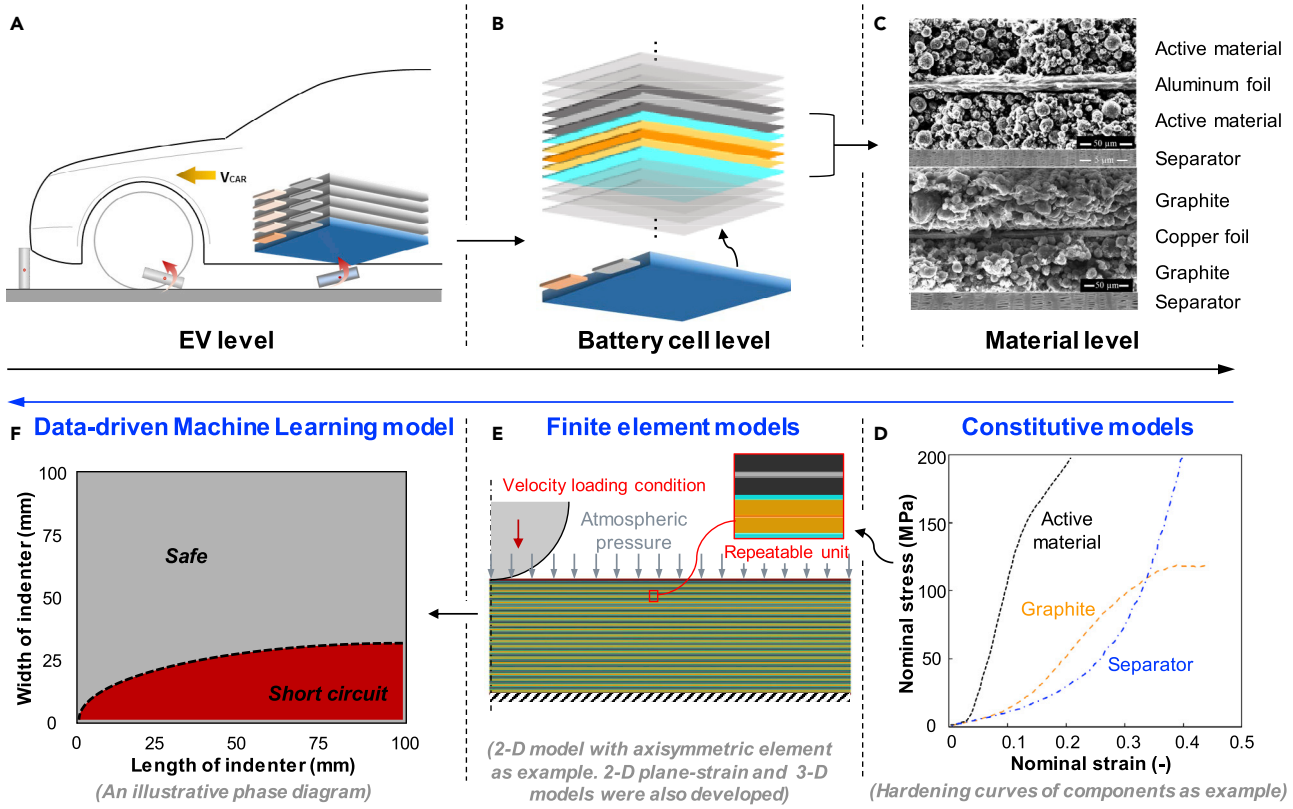

Figure 1. Multiple Scales of the Mechanical Safety Study and the Models at Each Scale

(A–C) The understanding of the problem is a "top-down" process: (A) EV – (B) battery cell – (C) components and materials. Scale bar, 5 μm for the separator image and 50 μm for the coating image.

(D–F) But the modeling adopts a "bottom-up" approach: constitutive models are developed at material level (D) and subsequently used as inputs for FE model (E), and the FE models generate big data for the development of data-driven ML models (F).

construction of the "safety envelope" of battery cells.[13] In realistic accidental scenarios, the battery cells may undergo various mechanical loading conditions (represented by the geometry and mass of the indenter, loading speed, loading direction, etc.), and it is, therefore, important to know the range of conditions ensuring safe operation of battery cells.

Creating the test matrix covering all the above types of loading and boundary conditions poses a formidable task. Performing hundreds or thousands of experiments is impossible even by a joint effort of academia and industry. The rapidly changing battery technology could make older tests obsolete as a new generation of cells comes to the market. The recently developed detailed computational model of cells offers a possibility of replacing the physical tests by the numerical simulations.[14] Such a model, released by the present investigating team, can predict with great realism all experimentally observed deformation and failure modes, including compaction, shear band localization, buckling, delamination, progressive fracture, and through-thickness crack formation, all leading to the development of the electric short circuit.

The only limitation for running a detailed finite element model is the cost of using, which comes not only from the runtime of submitting, running, and post-processing the computational simulations but also from the necessary training of a new user of the model. The former is almost inevitable unless a super-computer could be used, while the latter requires a good knowledge of mechanics of the user. Developing a

[1]Impact and Crashworthiness Lab, Massachusetts Institute of Technology, Cambridge, MA 02139, USA

[2]State Key Laboratory of Automotive Safety and Energy, Department of Automotive Engineering, Tsinghua University, Beijing 100084, China

[3]These authors contributed equally

[4]Lead Contact

*Correspondence: zhujuner@mit.edu (J.Z.), xiayong@tsinghua.edu.cn (Y.X.)

https://doi.org/10.1016/j.joule.2019.07.026

data-driven safety envelope overcomes these two limitations by means of creating a high-order table in which one can quickly look up the predictions with given loading situations and boundary conditions.

The issue is how to extract from a huge data bank trends and critical conditions of parameters leading to battery failure and the electric short circuit. Recent developments in the machine learning (ML) technique provides an effective tool to analyze big data. In the energy field, it has been used to seek the rational designs of energy materials[15–17] as well as to understand the mechanism of thermodynamic and electrochemical processes.[18–21] In this study, we will use this powerful tool to develop the safety envelope of lithium-ion pouch battery cells and show its possible applications in the EV and battery industries. The biggest challenge is that the ML approach requires a great amount of data on a certain type of battery cell, which, as mentioned earlier, are difficult to obtain solely by experiments. In particular, high-speed impact tests on high state-of-charge battery cells are dangerous and hard to be carried out. On the other hand, open literature is a good potential data resource of mechanical failure of commercial lithium-ion batteries, but data of "safe" battery tests have seldom been reported. Therefore, our present study adopts a more practical approach, which is studying the mechanical response of the battery under various loading conditions by numerical simulations.

Multi-scale Modeling of Commercial Lithium-Ion Batteries

The study of the mechanical safety of lithium-ion batteries involves multiple scales. Figure 1 shows the multi-scale modeling program[22] spanning three levels—EV (battery pack and module) level, battery cell level, and component material level. The understanding of the EV safety problem follows a "top-down" process from the macroscale to the microscale. More specifically, the accidental scenario happens at the EV level, but the mechanical deformation usually localizes at one individual cell, and the mechanical failure and the electric short circuit often initiate from several layers of electrodes at the material level. By contrast, the modeling program is a "bottom-up" procedure. The mechanical properties of the constituent materials should be tested and modeled as the basis for a successful finite element model of the whole battery cell. Subsequently, the cell-level model can be applied to the simulations of various loading conditions, generating data for the proposal of the data-driven safety envelope of battery cells that can be used for EV accident analysis in reality. The description of our modeling program adopts this bottom-up sequence.

Material Level: Testing and Constitutive Modeling

The present team developed, calibrated, validated, and implemented the detailed computational model of pouch cells. This model is used here as the tool to generate a large data bank of the output results. The interested reader is referred to the original publication.[14] Here, only a short outline of the method is given.

Mechanical tests were carried out on all the constituent materials of the battery cell in their dry conditions, including the graphite coating of the anode, the NMC coating of the cathode, the current collectors, the separator, and the polymer-coated aluminum pouch. Suitable constitutive models were selected according to the experimental results (see the summary in Table S1). The coatings are typical granular materials whose mechanical behavior depends on the hydrostatic pressure and exhibits a consolidation procedure subjected to compression (see Figure 1D), and therefore, the Drucker-Prager/Cap plasticity model was used (Figures S1–S4). The current collectors and the pouch are thin metal foils, so the J2 plasticity model with the Johnson-Cook ductile fracture criterion was adopted (Figure S5). The

separator is a highly porous polymeric film, and the crushable foam plasticity model was used. The strain rate dependence of the mechanical behavior of the component materials was investigated through tests under different loading speeds and modeled using a Johnson-Cook type function for the scaling of the hardening curve. In addition, our tests results showed that the dry stacked battery structure of the battery cell is almost rate insensitive, while the saturated sample by the electrolyte has an obvious rate dependence[23] (also see Figure S6). In other words, the rate dependence of the entire battery structure largely comes from the flow of electrolyte driven by the large deformation subjected to external loading and/or boundary conditions. In this current study, the electrolyte is not modeled directly as a real entity, but its effect is taken into consideration through the characterization of the rate dependence. The details of the testing and calibration process are described in the Supplemental Information.

Battery Cell Level: A High-Accuracy Finite Element Model

At the battery cell level, most of the finite element (FE) models existing in the literature are homogenized,[24–26] in which properties of all components were smeared into a continuum model, due to the complexity of the granular-metal multi-layered structure. However, to detect and locate the onset of the mechanical failure and electric short circuit, a detailed model that characterizes all the battery components (electrodes, current collectors, separators, and pouch) is necessary. The testing and modeling program carried out at the material level makes it possible to develop such a detailed model in Abaqus/explicit (see Figure 1E). Three modeling strategies are adopted (illustrated in Figure S7), which are 2D axisymmetric, 2D plane-strain, and the 3D full model. The former two have strict requirements for the loading conditions. The 2D axisymmetric model should be used when the indenter is a small object of revolution and the loading direction is perpendicular to the battery, and the 2D plane-strain model is suitable when the indenter is a long bar and the width of the battery cell is sufficiently greater than the thickness. Theoretically, the 3D full model can be used for all types of loading conditions (geometry of indenter and loading direction). All these three types of FE models share the same material constitutive relations as inputs, and the only difference lies in the element type of the code.

Two indentation tests at the cell level were carried out under the quasi-static loading condition as validations of the FE model. One indenter is a hemisphere with a radius of 6.5 mm, and the other is a cylindrical bar with a radius of 15 mm. The test setups and the force-displacement curve are shown in Figures 2A and 2B, respectively. It was found that the peak load coincides with the onset of the electric short circuit, measured by the drop in the voltage. At the same time, numerical simulations were carried out respectively using the 2D axisymmetric model and the 2D plane-strain model. The simulation results are plotted in the same coordinate for comparison. It is found that the correlation between simulation and experiments is almost perfect. More simulation results about strain localization could be found in Figure S8.

Moreover, high-resolution micro-CT scanning was performed to examine the fracture pattern of the tested battery cells, as shown in Figures 2C and 2D. In the hemispherical indentation test, the deformation is localized and fracture happens only in several layers near the surface, while in the cylindrical indentation, through-thickness cracks are observed. It should be noted that the fracture of both cases involves failure of the separator, which directly leads to the electric short circuit. The simulation results are also plotted in Figures 2C and 2D, where a very good correlation is observed. Particularly, the "X-shape" crack of the cylindrical indentation is successfully predicted. As mentioned above, 3D simulations were also performed as

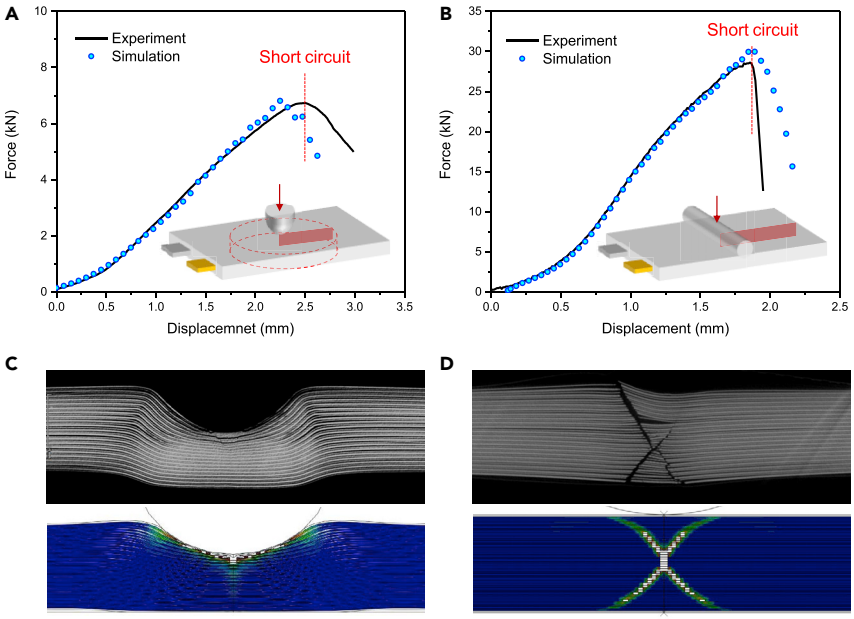

Figure 2. The Detailed FE Model Can Perfectly Match the Experimental Results

Two important aspects were investigated, force-displacement response (A and B) and fracture behavior (C and D). Two typical indentation scenarios were studied, hemispherical indentation (A and C) and cylindrical indentation (B and D). For both scenarios and both aspects, the agreement between simulations and experiments is almost perfect.

validation of our simulation strategy. The fracture pattern (Figure S9) and the force-displacement response (Figure S10) are compared to the 2D simulations, and an almost perfect agreement is achieved.

To sum up, the detailed FE model shows sufficient accuracy to predict both the force-displacement response and the fractured geometry of the lithium-ion pouch battery cell during indentations. It will now become a principal tool for generating simulation data under various loading conditions to study the safety of the battery cell. However, it should also be pointed out that high-speed dynamic tests were not performed on this type of battery cell due to the deficiency of the battery material and the lack of reliable experimental techniques, but it is clearly an important future study for the current research team.

EV Level: A Data-Driven Safety Envelope

In order to develop the data-driven safety envelope of lithium-ion battery cells, the problem should be parameterized, as shown in Figure 3. The geometry of the battery cell is described by the width W and the thickness H. Note that the length of the cell is not taken into consideration because usually, it is sufficiently larger than the width and consequently is not a critical dimension for the mechanical safety. The loading condition is described by the loading angle θ, the loading velocity v, and the mass of the indenter m. It is difficult to parameterize the geometry of the indenter because various objects of impact exist in realistic car accidents, and there is clearly no simple function that can universally describe all the possible geometries. In this study, the ellipsoid rigid indenter defined by R_1, R_2, and R_3 as the lengths of the three principal axes is adopted (see Figure 3). The advantage of this function is that most of the important loading cases can be covered. Particularly, $R_1=R_2=R_3$ represents the hemispherical indentation, $R_2=R_3 \ll R_1$ mimics the nail penetration test

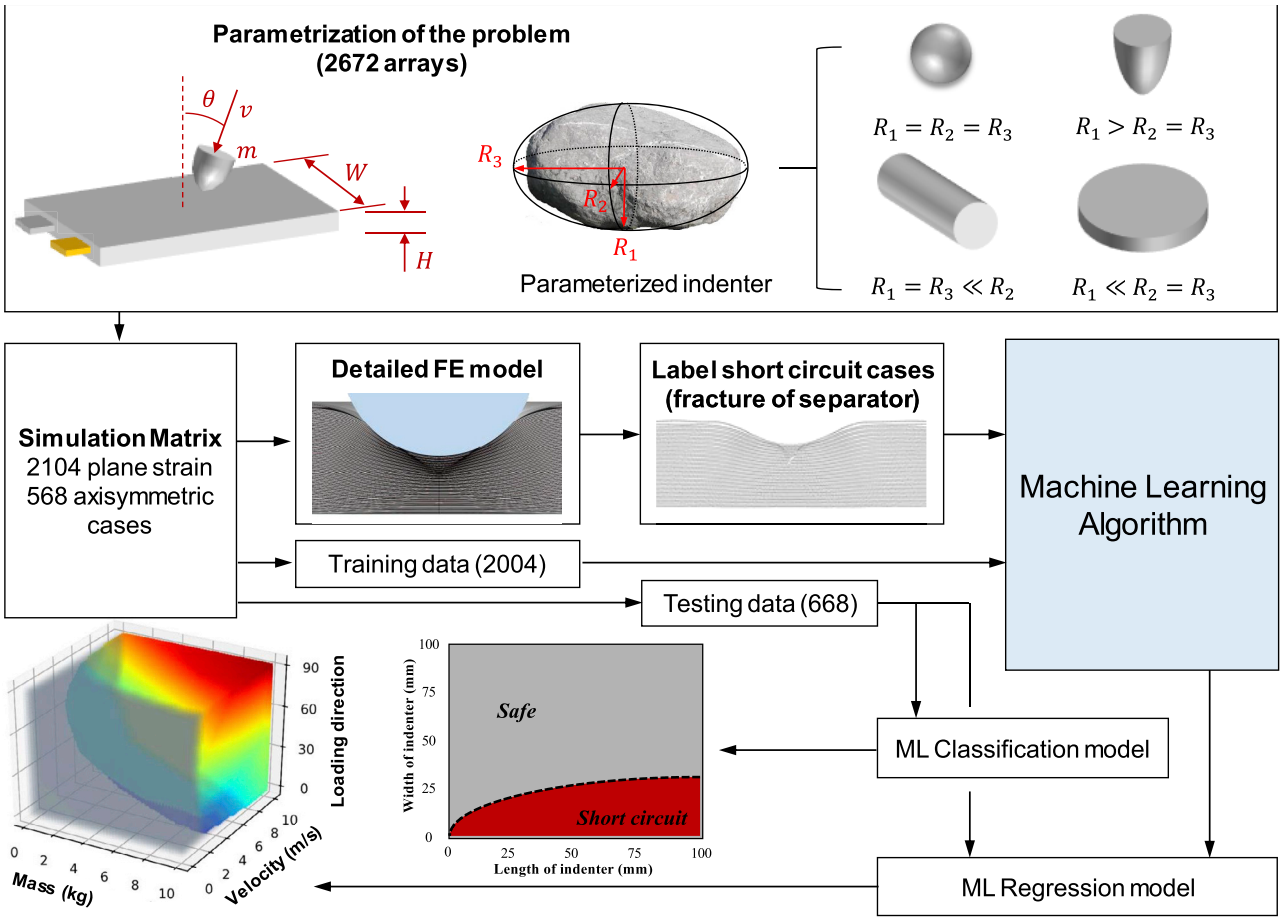

Figure 3. Flowchart of the Data-Driven Safety Envelope Using ML Algorithm

2,672 numerical simulations were conducted to generate data for the ML model. Fracture of the separator was used as a criterion of the electric short circuit. A classification model and a regression model were trained. The former is to predict short circuit, and the latter is to predict the intrusion of indenter to cause the short circuit.

that is currently used for safety evaluation, $R_1=R_3 \ll R_2$ generates a cylindrical bar indentation, and $R_1 \ll R_2=R_3$ characterizes the out-of-plane compression of the battery cell.

It is worth noting that there will be even more parameters if the material properties and the microstructures are varied from cell to cell. However, this study is focused on the influence of the loading condition, and therefore only the eight parameters introduced above were studied as variables. A simulation matrix of 2,672 arrays was then designed, which includes 2104 2-D plane-strain cases and 568 2-D axisymmetric cases (see Table S4). Only 2D cases were considered in the large matrix of simulations because of their higher computational efficiency than 3D simulations, and a small amount of 3D simulations were run to validate the results of the 2D ones (see the deformation and fracture pattern in Figure S9 and the force-displacement prediction in Figure S10). Three quarters of all the cases were used as training data for a certain ML algorithm, while the remainder as testing data. In all the numerical simulations, the fracture of the separator is used as a criterion to label the cases which end up with an electric short circuit[27] (see the labeled data in Figures S15–S17). The detection of this criterion as well as the data processing from Abaqus simulation to ML training and testing was realized by a Matlab code. The "safety

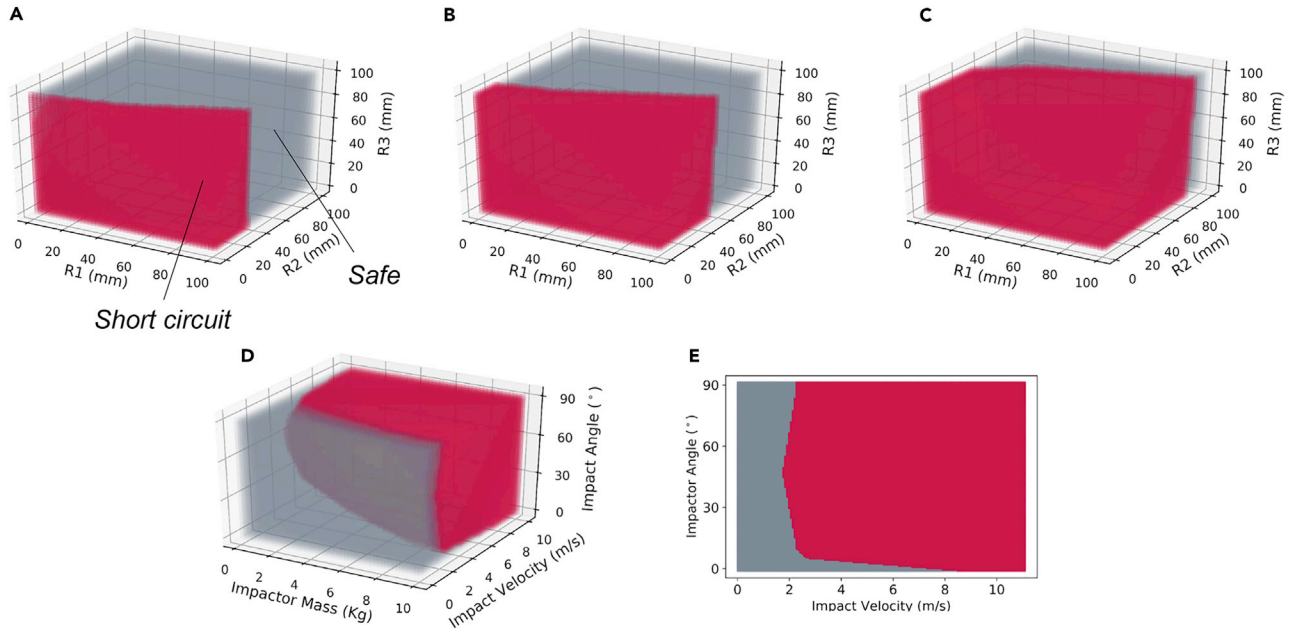

Figure 4. Classification Model of the Safety Envelope of the Studied Lithium-Ion Pouch Battery Cell

A set of phase diagrams of (R_1,R_2,*and* R_3) generated by the classification model at m = 4 kg, θ = 90° and different velocities (A) v = 4 m/s, (B) 6 m/s, and (C) 8 m/s shows that the safe and unsafe ranges of the shape of the indenter. On the other hand, a phase diagram of (m,v,θ) is obtained at R_1 = R_2 = R_3 = 6.35 mm (D) to show the effect of the loading condition, and a 2D plot (E) is exhibited at m = 10 kg to particularly show the effect of loading angle.

envelope" of the battery cell is characterized by two ML models, one classification model and one regression model. The former makes the quick judgment whether the given indenter and loading condition can lead to an electric short circuit, and the latter quantitatively predicts the intrusion, force, and kinetic energy of the indenter to cause a short circuit. Both models were trained with the same numerical simulation data bank independently. Three different ML algorithms, namely Decision Tree, Support Vector Machine (SVM), and Artificial Neural Network (ANN), were used for the classification, and the latter two were used for the regression because the Decision Tree algorithm is not suitable. A very detailed description and comparison of these three algorithms in the Supplemental Information (Figures S18–S22 for classification and Figures S23 and S24 for regression). Considering the accuracy of the prediction, the ANN with one hidden layer of 50 nodes and the SVM with RBF kernel are adopted for the classifier and the regressor, respectively.

RESULTS

Theoretically, the safety envelope of the studied lithium-ion battery cell is a complex function of the eight parameters involved. However, it is seen that there is a clearly difference in the sensitivity of the mechanical response to the eight different parameters. First, we found that the response has a very weak dependence on the two geometric variables of the battery cell, the thickness H and the width W (see Figure S11). Moreover, in reality, the values of these two variables are limited in a reasonable range, i.e. H is usually 5–10 mm, which is about 20 layers of alternating electrodes-separator units, and W is about 30–150 mm for the current EVs. Therefore, they are treated as insensitive variables, and the following safety envelope plots will be based on H = 6.72 mm and W = 30 mm. With this simplification, the problem only involves six variables with high sensitivity but it is still almost impossible to visualize the safety envelope completely in one coordinate. A convenient and practical visualization approach is the 3D "phase diagrams" by choosing three of the six

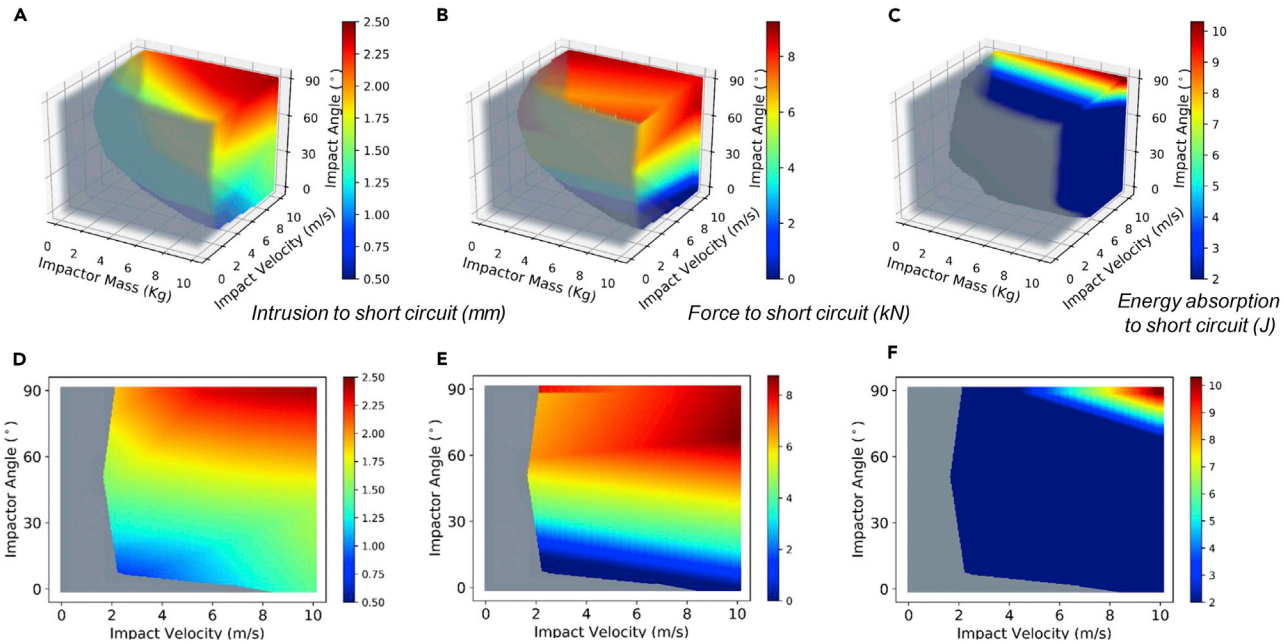

Figure 5. Regression Model of the Safety Envelope of the Studied Lithium-Ion Pouch Battery Cell

(A–C) Based on Figure 4D at $R_1 = R_2 = R_3 = 6.35$ mm, the "unsafe" range is specified with the contour of the (A) intrusion of the indenter, (B) resistive force, and (C) energy absorption of the battery cell to the short circuit.

(D–F) The 2D plots for (D), (E), and (F) are obtained from (A), (B), and (C), respectively, at $m = 10$ kg.

parameters as variables and fixing the others at realistic values. Phase diagrams of (R_1,R_2,*and* R_3) are plotted in Figures 4A–4C at fixed mass $m = 4$ kg, loading angle $\theta = 90°$ and three different velocities (a) $v = 4$ m/s, (b) 6 m/s, and (c) 8 m/s, respectively. If the battery cell is deformed by an indenter with R_1, R_2, and R_3 that is in the red range, an electric short circuit will be caused. Otherwise, it is mechanically safe (gray range). Clearly, a sharp indenter (small R_2 and large R_1 and R_3) is more dangerous to the battery than blunt ones. Besides, as the loading velocity increases, the range of short circuit becomes wider, which agrees well with the well-known rule of impact crashworthiness that high impact energy is dangerous to a structure.

Phase diagrams choosing the mass of the indenter m, the loading velocity v, and the loading angle θ as variables show the effect of the loading condition. Figure 4D presents an exemplary diagram obtained at $R_1 = R_2 = R_3 = 6.35$ mm. One clear conclusion is that the short circuit is more likely to happen when the impact energy ($mv^2/2$) of the indenter is high. Interestingly, the dependence on the load angle θ is complicated. Therefore, a 2D plot is constructed at the impact mass of 10 kg and is shown in Figure 4E. An interesting observation is that the vertical loading (90°) is not necessarily the most critical loading direction. When the impact indentation happens in about 50°, a smaller velocity (1.9 m/s) is needed to cause the electric short circuit compared to the 2.2 m/s in 90°. This finding is of great importance to the safety testing of lithium-ion battery cells, and more discussions will be provided in the following section.

The regression model can not only show the ranges of the safe and electric short circuit ranges but also quantitatively predict the amount of intrusion, force, and energy absorption to which the short circuit happens. Figure 5 shows the (m,v,*and* θ) diagram at $R_1 = R_2 = R_3 = 6.35$ mm with respect to the intrusion of the indenter, the reactive force on the indenter, and the energy absorption, respectively. Clearly, these three

quantities vary greatly with the change of loading conditions, which indicates that the short circuit is a complex phenomenon of the interplay of the amount of intrusion, reactive force, and kinetic energy, etc. In other words, the prediction of the short circuit of a lithium-ion battery cell cannot be realized by a fixed single-value criterion of the intrusion, the reactive force, or kinetic energy of the indenter. This is because the underlying physical mechanism is the contact of the anode and the cathode through the fracture of the separator, which is a complex process involving the failure strain of the separator, the architecture of the whole battery cell, the mechanical properties of all the component materials, and the boundary conditions. The finding justifies the motivation of the development of the safety envelope of the present study. Another conclusion from the results in Figures 5C and 5F is that the lithium-ion battery cell itself is not a good energy absorber, particularly when subjected to an oblique impact loading. This characteristic of the cell emphasizes the importance of designing additional ballistic protective structures to absorb the kinetic energy of the indenter.[28]

DISCUSSION

Applications of the Safety Envelope

The Most Critical Loading Condition

One of the major advantages of the data-driven safety envelope over the FE model is that the data can be analyzed to identify the common parameters that lead most likely to battery failure, i.e., the identification of a non-obvious trend. The first important application of the safety envelope is the identification of the most critical loading condition such that protective structures can be designed accordingly. The results of this study revealed that the risk of an electric short circuit monotonically increases with the increase of R_1, R_3, m, and v and the decrease of R_2. In other words, sharp impact objects with large impact energy are always more dangerous. However, the most critical loading angle exists as indicated by the safety envelope, which is between 50° to 60° as revealed previously. This special phenomenon is largely due to the internal friction of the battery structure, which comes from two sides. First, the granular coatings are typical frictional materials in which the particles can slide between one another.[29] Through our tests, it was found that the mechanical property of the granular coatings, the friction angle of which is around 60°–70°, which is dependent on the content of binder and carbon black.[30] In other words, the granular coatings of the electrodes tend to break more easily when the loading angle is in this range.[31] The second source of the internal friction of the battery structure is the frictional interface between the separator and the electrode coatings. According to our tests, the frictional coefficient is around 0.4, which is approximately 21.8° in terms of friction angle. The overall friction angle of the battery structure is therefore the combination of these two sources, while the friction of the granular coatings has a larger contribution because the materials occupy the majority of the structure. As an estimation, the friction angle of the whole battery cell should be around 60°, which gives a reasonable explanation of the most critical loading angle revealed by the safety envelope. The fracture pattern under 60° plane-strain indentation is shown in Figure S25, where the angle between the fracture plane and the battery horizontal plane is also approximately 60°. It should be pointed out that dynamic indentation tests in different loading directions are needed to experimentally validate this observation, but it was found that this test is extremely challenging. On one hand, the difference in the critical velocity (1.9 m/s for 50° and 2.2 m/s for 90°) is so small that a high accuracy of the speed-control system is required. Therefore, the conventional gravity-based drop mass loading machine is not a good option. On the other hand, the result of an oblique impact loading in reality is often affected by a slippery between the indenter and the pouch, which can introduce a large amount of uncertainty for the measurements. For these two reasons, experimental validation of the safety envelope is a clear candidate for the future research.

Passive Safety: Design of Protective Structures of Battery Modules

Knowing what the most critical loading condition is can greatly help the design of the protective structures of the battery module and pack. The safety envelope of the studied battery cell provides two guidelines: (1) absorbing sufficient kinetic energy from the impact object and (2) deflecting the object (changing the loading direction). The former can be realized by introducing stiff prismatic members and energy-absorbing materials such as foam, honeycomb, and sandwich structures,[11,28] while the latter was introduced by re-designing the Tesla Model S after two highly publicized fire accidents in 2013.[32] The protective barriers were added to deflect a possible indenter coming from the road.

Active Safety: Incorporating the Safety Envelope into Vehicle CPUs

The safety envelope developed in the current study is purely data driven so that it can be easily incorporated into the central processing unit (CPU) of EVs. On a vehicle equipped with a sufficient sensor system to detect the loading condition of an external object (geometry, mass, loading speed, and angle), the developed safety envelope could provide a prediction of the safety of lithium-ion battery cells. As mentioned above, this prediction process reduces the computational runtime and is therefore very fast, which is essential to the applications in the active safety system as well as the autonomous vehicles in the future.

Standardization of Battery Safety Tests

One of the difficulties for the assessment of battery safety is due to the absence of a standard test that would be accepted worldwide by different investigating teams, companies, and countries.[10] For example, our MIT team has proposed several typical tests such as the cylindrical indentation and hemispherical indentation described above,[26,33,34] and the Oak Ridge National Lab (ORNL) is using the pinching tests.[35,36] Besides, the nail penetration test has been used by many organizations for the study of thermal runaway, particularly including the China government.[6,37–39] In this type of test, the conductivity of the indenter (nail) plays an important role. The existence of these various tests makes it difficult to compare different batteries and collect data for the development of the safety envelope. To standardize the mechanical safety tests, the most critical and representative loading condition should be found. According to our safety envelope, we recommend that the local indentation test with sharp and blunt indenters in 50°–60° at a high loading speed (e.g., 1–5 m/s) can be used as a standard safety test of the commercial lithium-ion battery cells. Further researches and discussions are required to determine the specific geometry of the indenter.

Limitations and Outlooks

It should be noted that the present study does have some limitations. First, the safety envelope was developed for one type of battery cell (large-format secondary pouch cell with NMC cathode and graphite anode) and is therefore not universal. Second, the data used for the safety envelope comes from numerical simulations and always carries errors as compared to the real world. However, it is a needed compromise due to the large cost of an experimental program. Especially, dynamic tests were not performed as validation in this current study, which clearly can be an important next step for the future. Third, the two important dependences of the mechanical behavior were not taken into consideration, one on the state of charge of the cell and the other on the wetting of electrolyte. Both of them could substantially influence the mechanical property of some components. For example, some certain types of separators may become softer in the electrolyte due to the interaction between the polymer chain of the separator and the molecules of the electrolyte

according to some existing studies.[40] Last, variables from the material and structure of the battery cell, such as the number of layers, thickness, and strength of each component and the existence of liquid electrolyte were not taken into consideration. Therefore, the current study serves as a demonstration of the application of the ML tool in the development of safety models of EV lithium-ion battery cells, and the improvement of this study can be expected on these three aspects.

EXPERIMENTAL PROCEDURES

Material Testing

Raw materials, (NMC powders, graphite powders, carbon black, copper foils, aluminum foils, and binder) were obtained from the industrial sponsors of the MIT Battery Modeling Consortium. The mechanical tests of coatings started from the preparation of disk samples, which includes the mixing of slurry, die casting, drying, and pre-compression to a wanted density (to mimic the calendaring process). The procedure is described in Figure S1. Axial compression, lateral compression, and closed-die compaction tests were carried out to calibrate the mechanical model of coatings (Figure S2). For the metal foils (current collectors) and separators, samples with different geometries were cut from the commercial battery foils and tested with an Instron 5944 testing machine. High-speed mechanical tests were carried out by the Automotive Crash Lab at Tsinghua University.

Indentation Tests of the Battery Cells

A batch of large-format EV battery cells was obtained from the industrial sponsors, and some small-format ones were produced in the MIT lab using the same raw materials. The mechanical behavior of these two batches of batteries was found to be almost identical. Indentations tests were carried out using an MTS loading machine with a 200 kN load cell. The loading speed was 6 mm/min. The displacement of the indenters was measured by the Digital Image Correlation approach with a CCD camera.

FE Simulations

Simulations were carried out using Abaqus/explicit with 8 CPUs. Element types CAX4R, CPE4R, and C3D8R are used respectively for 2D axisymmetric, 2D plane-strain, and 3D models. The total number of elements is 21,000 for the 2-D axisymmetric model, 42,000 for the 2D plane-strain, and 10,000,000 for the 3D. Frictional contact with a frictional coefficient of 0.4 is defined between the coatings and the separator, and the interface between the coatings and the current collectors is the surface-to-surface tie.

ML Algorithm

Three different ML algorithms, namely the Decision Tree (Figures S12 and S18), Support Vector Machine (SVM, Figures S13, S18–S20, and S24), and Artificial Neural Network (ANN, Figures S14 and S21–S23), were used in the present study, all of which have been proven to be effective to analyze big data and therefore have already been widely used. Among them, ANN and SVM can solve both classification and regression problems, but the Decision Tree algorithm can only be applied to classification problems. All the three algorithms were used for the classification model in our study to predict whether the battery will fail or not for a given loading condition. It was found that both SVM with RBF (radial basis function) kernel and ANN give satisfactory predictions. We selected the ANN with one hidden layer of 50 nodes for the classification model because its accuracy turned out to be slightly higher in this certain case. For the regression problem, we compared ANN and SVM. It was found that SVM can provide much more accurate prediction than ANN can. Therefore, SVM with RBF kernel is used for the regression model in our study. A

possible reason for this comparison result is that it is convenient to tune the parameters of SVM algorithm to avoid overfitting. The models were developed with the open-source neural-network library Keras and the ML library scikit-learn in Python. More details are described in the Supplemental Information.

SUPPLEMENTAL INFORMATION

Supplemental Information can be found online at https://doi.org/10.1016/j.joule.2019.07.026.

ACKNOWLEDGMENTS

The financial support from the MIT Battery Modeling Consortium (Altair, AVL, Boston-Power, Dassault Systèmes Simulia, Jaguar-Land Rover, LG Chem, Mercedes-Benz, Murata, and PSA Groupe), the International Science & Technology Cooperation Program of China (grant no. 2016YFE0102200), and the National Natural Science Foundation of China (grant no. 51675294) is gratefully acknowledged. Thanks are due to Ford Motor Company for partial financial support. In addition, the partial support from the USAID SHERA Program is acknowledged. W.L. thanks the China Scholarship Council (CSC) for the visiting student scholarship during his stay at MIT. J.Z. would like to thank Professor Martin Bazant, Professor W Craig Carter, Professor Ken Kamrin, and Professor Elham Sahraei for their constructive comments. All the authors thank Dr. Jonathon Harding at Exponent Inc. for performing the micro CT imaging of the damaged battery cells.

AUTHOR CONTRIBUTIONS

J.Z., W.L., and T.W. conceived the idea. J.Z. and Y.X. designed the research. W.L. and J.Z. performed the experiments. W.L. ran numerical simulations and post-processed all the data. W.L. and M.G. developed the ML model. T.W. and Y.X. secured funding. J.Z. and W.L. prepared the manuscript as well as the Supplemental Information, and all authors contributed to the writing and revising of the manuscript.

DECLARATION OF INTERESTS

The authors declare no competing interests.

Received: May 8, 2019
Revised: June 3, 2019
Accepted: July 24, 2019
Published: August 26, 2019

REFERENCES

1. Tarascon, J.M., and Armand, M. (2001). Issues and challenges facing rechargeable lithium batteries. Nature *414*, 359–367.

2. Schmuch, R., Wagner, R., Hörpel, G., Placke, T., and Winter, M. (2018). Performance and cost of materials for lithium-based rechargeable automotive batteries. Nat. Energy *3*, 267–278.

3. Kwade, A., Haselrieder, W., Leithoff, R., Modlinger, A., Dietrich, F., and Droeder, K. (2018). Current status and challenges for automotive battery production technologies. Nat. Energy *3*, 290–300.

4. Liu, X., Ren, D., Hsu, H., Feng, X., Xu, G.L., Zhuang, M., Gao, H., Lu, L., Han, X., Chu, Z., et al. (2018). Thermal runaway of lithium-ion batteries without internal short circuit. Joule *2*, 2047–2064.

5. Abada, S., Marlair, G., Lecocq, A., Petit, M., Sauvant-Moynot, V., and Huet, F. (2016). Safety focused modeling of lithium-ion batteries: a review. J. Power Sources *306*, 178–192.

6. Finegan, D.P., Tjaden, B., Heenan, T.M.M., Jervis, R., Michiel, M.D., Rack, A., Hinds, G., Brett, D.J.L., and Shearing, P.R. (2017). Tracking internal temperature and structural dynamics during nail penetration of lithium-ion cells. J. Electrochem. Soc. *164*, A3285–A3291.

7. Walker, W.Q., Darst, J.J., Finegan, D.P., Bayles, G.A., Johnson, K.L., Darcy, E.C., and Rickman, S.L. (2019). Decoupling of heat generated from ejected and non-ejected contents of 18650-format lithium-ion cells using statistical methods. J. Power Sources *415*, 207–218.

8. Feng, X., Ouyang, M., Liu, X., Lu, L., Xia, Y., and He, X. (2018). Thermal runaway mechanism of lithium ion battery for electric vehicles: a review. Energy Storage Mater. *10*, 246–267.

9. Rodrigues, M.F., Babu, G., Gullapalli, H., Kalaga, K., Sayed, F.N., Kato, K., Joyner, J., and Ajayan, P.M. (2017). A materials perspective on Li-ion batteries at extreme temperatures. Nat. Energy *2*, 17108.

10. Ruiz, V., Pfrang, A., Kriston, A., Omar, N., Van den Bossche, P., and Boon-Brett, L. (2018). A review of international abuse testing standards and regulations for lithium ion batteries in

electric and hybrid electric vehicles. Renew. Sustain. Energy Rev. *81*, 1427–1452.

11. Xia, Y., Wierzbicki, T., Sahraei, E., and Zhang, X. (2014). Damage of cells and battery packs due to ground impact. J. Power Sources *267*, 78–97.
12. Deng, J., Bae, C., Marcicki, J., Masias, A., and Miller, T. (2018). Safety modelling and testing of lithium-ion batteries in electrified vehicles. Nat. Energy *3*, 261–266.
13. Narayana Prasad, A. (2018). Engineering Safety Analysis of EV Li-Ion Batteries for Mini Zing Auto Insurance Losses, Doctroal thesis (Massachusetts Institute of Technology). http://hdl.handle.net/1721.1/118534.
14. Zhu, J., Li, W., Wierzbicki, T., Xia, Y., and Harding, J. (2019). Deformation and failure of lithium-ion batteries treated as a discrete layered structure. Int. J. Plast.
15. Correa-Baena, J.P., Hippalgaonkar, K., van Duren, J., Jaffer, S., Chandrasekhar, V.R., Stevanovic, V., Wadia, C., Guha, S., and Buonassisi, T. (2018). Accelerating materials development via automation, machine learning, and high-performance computing. Joule *2*, 1410–1420.
16. Lopez, S.A., Sanchez-Lengeling, B., de Goes Soares, J., and Aspuru-Guzik, A. (2017). Design principles and top non-fullerene acceptor candidates for organic photovoltaics. Joule *1*, 857–870.
17. Nolan, A.M., Zhu, Y., He, X., Bai, Q., and Mo, Y. (2018). Computation-accelerated design of materials and interfaces for all-solid-state lithium-ion batteries. Joule *2*, 2016–2046.
18. Brandt, R.E., Kurchin, R.C., Steinmann, V., Kitchaev, D., Roat, C., Levcenco, S., Ceder, G., Unold, T., and Buonassisi, T. (2017). Rapid photovoltaic device characterization through bayesian parameter estimation. Joule *1*, 843–856.
19. Howard, J.M., Tennyson, E.M., Neves, B.R.A., and Leite, M.S. (2019). Machine learning for perovskites' reap-rest-recovery cycle. Joule *3*, 325–337.
20. Mao, Y., Wang, X., Xia, S., Zhang, K., Wei, C., Bak, S., Shadike, Z., Liu, X., Yang, Y., Xu, R., et al. (2019). High-voltage charging-induced strain, heterogeneity, and micro-cracks in secondary particles of a nickel-rich layered cathode material. Adv. Funct. Mater. *29*, 1900247.
21. Severson, K.A., Attia, P.M., Jin, N., Perkins, N., Jiang, B., Yang, Z., Chen, M.H., Aykol, M., Herring, P.K., Fraggedakis, D., et al. (2019). Data-driven prediction of battery cycle life before capacity degradation. Nat. Energy *4*, 383–391.
22. Zhu, J., Wierzbicki, T., and Li, W. (2018). A review of safety-focused mechanical modeling of commercial lithium-ion batteries. J. Power Sources *378*, 153–168.
23. Zhu, J., Luo, H., Li, W., Gao, T., Xia, Y., and Wierzbicki, T. (2019). Mechanism of strengthening of battery resistance under dynamic loading. Int. J. Impact Eng. *131*, 78–84.
24. Wierzbicki, T., and Sahraei, E. (2013). Homogenized mechanical properties for the jellyroll of cylindrical lithium-ion cells. J. Power Sources *241*, 467–476.
25. Greve, L., and Fehrenbach, C. (2012). Mechanical testing and macro-mechanical finite element simulation of the deformation, fracture, and short circuit initiation of cylindrical lithium ion battery cells. J. Power Sources *214*, 377–385.
26. Chung, S.H., Tancogne-Dejean, T., Zhu, J., Luo, H., and Wierzbicki, T. (2018). Failure in lithium-ion batteries under transverse indentation loading. J. Power Sources *389*, 148–159.
27. Zhang, X., Sahraei, E., and Wang, K. (2016). Deformation and failure characteristics of four types of lithium-ion battery separators. J. Power Sources *327*, 693–701.
28. Zhu, J., Zhang, X., Wierzbicki, T., Xia, Y., and Chen, G. (2018). Structural designs for electric vehicle battery pack against ground impact. vol. 2018-April. SAE Tech. Pap.
29. Anand, L., and Gu, C. (2000). Granular materials: constitutive equations and strain localization. J. Mech. Phys. Solids *48*, 1701–1733.
30. Zhu, J., Li, W., Xia, Y., and Sahraei, E. (2018). Testing and modeling the mechanical properties of the granular materials of graphite anode. J. Electrochem. Soc. *165*, A1160–A1168.
31. Kamrin, K., and Bazant, M.Z. (2007). Stochastic flow rule for granular materials. Phys. Rev. E Stat. Nonlinear Soft Matter Phys. *75*, 041301.
32. Musk, E. (2014). Tesla adds titanium underbody shield and aluminum deflector plates to model S. https://www.tesla.com.
33. Sahraei, E., Bosco, E., Dixon, B., and Lai, B. (2016). Microscale failure mechanisms leading to internal short circuit in Li-ion batteries under complex loading scenarios. J. Power Sources *319*, 56–65.
34. Sahraei, E., Campbell, J., and Wierzbicki, T. (2012). Modeling and short circuit detection of 18650 Li-ion cells under mechanical abuse conditions. J. Power Sources *220*, 360–372.
35. Wang, H., Watkins, T.R., Simunovic, S., Bingham, P.R., Allu, S., and Turner, J.A. (2017). Fragmentation of copper current collectors in Li-ion batteries during spherical indentation. J. Power Sources *364*, 432–436.
36. Wang, H., Simunovic, S., Maleki, H., Howard, J.N., and Hallmark, J.A. (2016). Internal configuration of prismatic lithium-ion cells at the onset of mechanically induced short circuit. J. Power Sources *306*, 424–430.
37. Mao, B., Chen, H., Cui, Z., Wu, T., and Wang, Q. (2018). Failure mechanism of the lithium ion battery during nail penetration. Int. J. Heat Mass Transf. *122*, 1103–1115.
38. Hatchard, T.D., Trussler, S., and Dahn, J.R. (2014). Building a "smart nail" for penetration tests on Li-ion cells. J. Power Sources *247*, 821–823.
39. Finegan, D.P., Darst, J., Walker, W., Li, Q., Yang, C., Jervis, R., Heenan, T.M.M., Hack, J., Thomas, J.C., Rack, A., et al. (2019). Modelling and experiments to identify high-risk failure scenarios for testing the safety of lithium-ion cells. J. Power Sources *417*, 29–41.
40. Sheidaei, A., Xiao, X., Huang, X., and Hitt, J. (2011). Mechanical behavior of a battery separator in electrolyte solutions. J. Power Sources *196*, 8728–8734.